Mechanism for Cavitation Phenomenon in Mechanical Heart Valves

Hwansung Lee*, Yoshiyuki Taenaka
Department of Artificial Organs, Research Institute, National Cardiovascular Center, 5-7-1 Fujishiro-dai, Suita, Osaka 565-8565, Japan

Recently, cavitation on the surface of mechanical heart valve has been studied as a cause of fractures occurring in implanted Mechanical Heart Valves (MHVs). It has been conceived that the MHVs mounted in an artificial heart close much faster than in vivo sue, resulting in cavitation bubbles formation. In this study, six different kinds of monoleaflet and bileaflet valves were mounted in the mitral position in an Electro-Hydraulic Total Artificial Heart (EHTAH), and we investigated the mechanisms for MHV cavitation. The valve closing velocity and a high speed video camera were employed to investigate the mechanism for MHV cavitation. The closing velocity of the bileaflet valves was slower than that of the monoleaflet valves. Cavitation bubbles were concentrated on the edge of the valve stop and along the leaflet tip. It was established that squeeze flow holds the key to MHV cavitation in our study. Cavitation intensity increased with an increase in the valve closing velocity and the valve stop area. With regard to squeeze flow, the bileaflet valve with slow valve-closing velocity and small valve stop areas is better able to prevent blood cell damage than the monoleaflet valves.

Key Words: Artificial Heart, Mechanical Heart Valve, Cavitation Bubble, Squeeze Flow

Nomenclature

h : Gap between a leaflet and valve stop (mm)
L : Length of the valve stop (mm)
V : Valve-closing velocity (m/s)
P : Pressure (Pa)
U : Squeeze flow velocity (m/s)
μ : Fluid viscosity (Pa·s)
ρ : Density of fluid (g/cm^3)

1. Introduction

When cavitation occurs near the material surface of a mechanical heart valve, this rapid collapse may cause the generation of a high speed micro-jet and shock waves, resulting in the generation of high pressure. This high pressure causes pitting and erosion on the leaflet (Klepetko, 1989; Kafesjian, 1994), and is a plausible source of traumatic blood damage (Graf, 1992; Garrison, 1994). Therefore, cavitation in mechanical heart valves has been widely studied (Garrison, 1994; He, 2001; Lee, 1996; Sneckenberger, 1996; Wu, 1994; Makhijani, 1994; Graf, 1994). In order for cavitation bubbles to grow, the pressure must fall below the vapor pressure for a limited period of time (Knapp, 1979). If the length of time that the pressure falls below the vapor pressure is too long, the cavitation bubbles will grow too large. The larger the cavitation bubbles, the higher the pressure that is generated when these bubbles collapse. Therefore, in order to quantify Mechanical Heart Valve (MHV) cavitation, the cavitation existing time is induced as the cavitation intensity.

In general, the major causes of cavitation in mechanical heart valves included the venturi effect due to flow after valve closure in the narrow gap

* Corresponding Author,
E-mail: hslee@ri.ncvc.go.jp
TEL: +81-6-6833-5004 (ext.2368);
FAX: +81-6-6835-5406
Department of Artificial Organs, Research Institute, National Cardiovascular Center, 5-7-1 Fujishiro-dai, Suita, Osaka 565-8565, Japan. (Manuscript **Received** January 25, 2005; **Revised** May 25, 2006)

between the leaflet and valve housing, the water hammer effect due to the sudden stop of MHV leaflets, and the squeeze flow that can occur in the narrow gap between the leaflet and valve stop (Wu, 1994; Makhijani, 1994; Graf, 1994). In previous studies, erosion pits due to cavitation have been shown to be restricted to an area on the valve surface next to the edge of the valve stop where squeeze flow occurs. Squeeze flow occurs just before valve closure, which contributes to MHV cavitation (Lee, 1996; Bluestein, 1994; He, 2001).

In this study, in order to investigate the mechanisms of MHV cavitation with an electro-hydraulic total artificial heart (EHTAH), the valve-closing velocity and a high speed video camera were employed.

2. Materials and Methods

The electro-hydraulic totally artificial heart (EHTAH) with a stroke volume of 75-80 ml was developed by the National Cardiovascular Center in Japan (Fig. 1); this heart model consists of two diaphragm-type blood pumps, an actuator, and a controller. The actuator is connected to both blood pumps by flexible tubes. The flexible tubes are filled with silicon oil. This EHTAH system functions as follows: silicon oil drives the blood pump via the inverse and/or reverse rotation of the impeller. The EHTAH was connected to a mock circulatory loop tester. As the pressure condition, the mean left atrium and mean aortic pressure were maintained the same as normal physiology condition.

Three kinds of monoleaflet valves and three kinds of bileaflet valves were used (Fig. 2 and Table 1). These various mechanical heart valves were mounted in the mitral position. As the working fluid, we used a 50% aqueous glycerin solution at 37℃ (50% glycerin by volume in distilled water) which had a viscosity coefficient of 0.0034

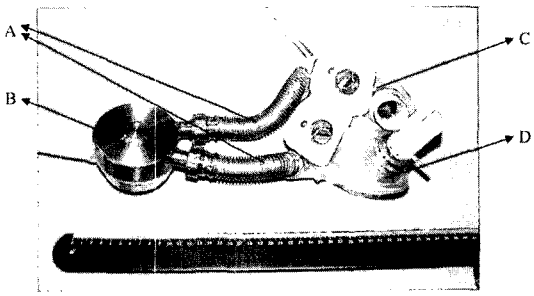

Fig. 1 An electro-hydraulic total artificial heart. (A) Flexible tube, (B) Actuator, (C) Left blood pump, (D) Right blood pump

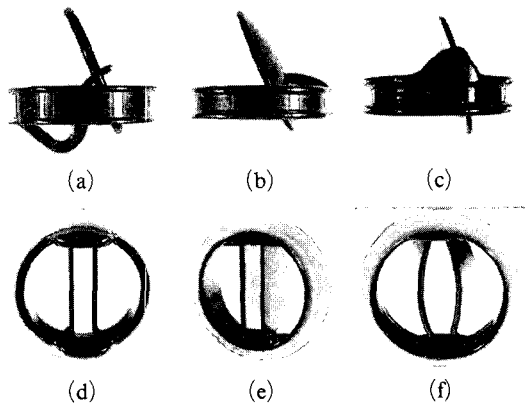

Fig. 2 Photographs of the mechanical heart valve. (a) Medtronic Hall valve, (b) Björk-Shiley valve, (c) Omnicarbon valve, (d) St. Jude valve, (e) ATS valve, (f) Sorin valve

Table 1 Prosthetic heart valves used in this study

Valves	Type	Outer diameter	Orifice diameter	Opening angle
Medtronic Hall valve	Monoleaflet	25 mm	20 mm	70 degrees
Björk-Shiley valve	Monoleaflet	25 mm	20 mm	70 degrees
Omnicarbon valve	Monoleaflet	23 mm	18 mm	68 degrees
St. Jude valve	Bileaflet	21 mm	14.7 mm	58 degrees
ATS valve	Bileaflet	21 mm	14.8 mm	60 degrees
Sorin valve	Bileaflet	21 mm	15.2 mm	60 degrees

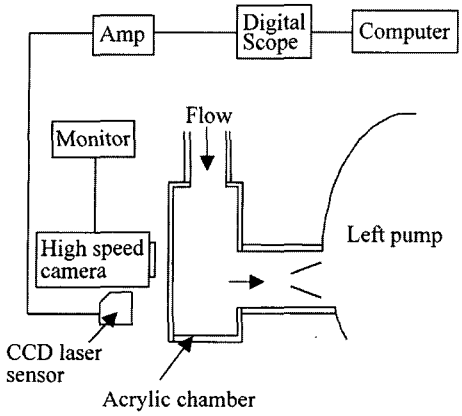

Fig. 3 Diagram of the experimental system

Pa·s, a density of 1.12 g/cm^3, and a vapor pressure of −95.3 kPa. In other words, its fluid viscosity and vapor pressure were identical to those of blood at body temperature.

The EHTAH was run at a heart rate ranging from 60 to 100 beats/min, and the cardiac outputs ranged from 4.5 to 7.5 L/min. The filling and eject conditions of the left blood pump were controlled by changing the heart rate, left systolic ratio and motor revolution speed. The left pump was maintained the full filling and full eject conditions. The left systolic ratio was 48%, and the motor revolution speed ranged between 1,300 and 1,700 rpm for the left systole, and 1,100 and 1,500 rpm for the right systole.

Cavitation bubbles were recorded at 20,000 frames per second with a high speed video camera (Memrecam fx 6000, nac, Tokyo, Japan). A CCD laser displacement sensor (LC-2450, Keyence, Osaka, Japan) with a resonance frequency of 50 kHz was used to detect the valve closing motion just before closure.

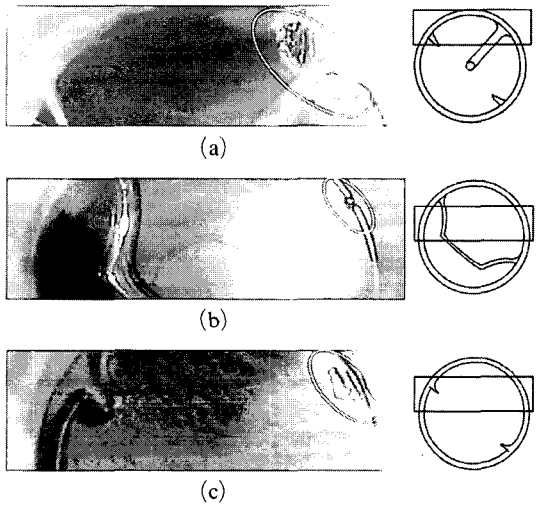

Fig. 4 Cavitation bubbles in the monoleaflet valves. (a) Medtronic Hall valve, (b) Björk-Shiley valve, (c) Omnicarbon valve

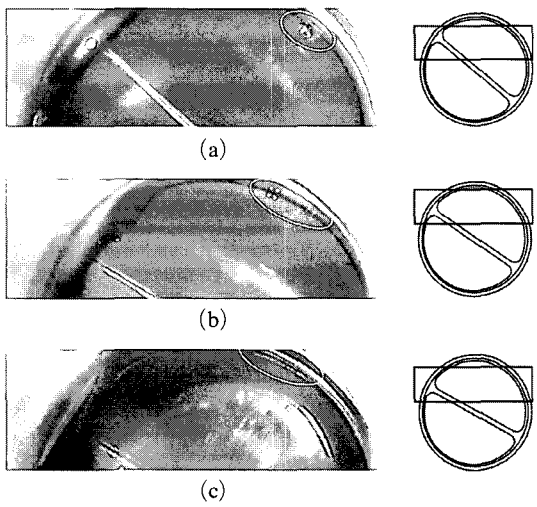

Fig. 5 Cavitation bubbles in the bileaflet valves. (a) St. Jude valve, (b) ATS valve, (c) Sorin valve

3. Results

Cavitation bubbles in the Medtronic Hall valve with a heart rate of 90 beats/min were concentrated on the edge of the valve stop (Fig. 4(a)). In the Omnicarbon valve with a heart rate of 90 beats/min, cavitation bubbles were observed along the leaflet tip (Fig. 4(b)). Its cavitation bubbles were occurred by squeeze flow. Cavitation bubbles in the Björk-Shiley valve with a heart rate of 90 beats/min were observed in the narrow gap between the leaflet and valve housing (Fig. 4 (c)), which is cause by venturi effect.

In the three kinds of bileaflet valves, using a heart rate of 90 beats/min, most of the cavitation bubbles were concentrated along the leaflet tip. There was a significant difference in the cavitation intensity, however, the mechanism for cavi-

Table 2 The valve closing velocity at 0.5 ms just before valve closure

Heart rate (beats/min)	Monoleaflet valves (m/s)			Bileaflet valves (m/s)		
	MH	BS	OC	SJ	ATS	Sorin
60	3.01±0.31	2.02±0.22	2.10±0.21	1.50±0.30	1.73±0.40	1.60±0.21
70	3.46±0.40	2.31±0.20	2.38±0.50	1.74±0.45	2.38±0.41	1.80±0.25
80	3.85±0.40	2.46±0.32	3.07±0.42	2.05±0.40	2.50±0.40	2.01±0.31
90	4.19±0.42	3.02±0.31	3.46±0.44	2.06±0.42	2.61±0.43	2.60±0.32
100	4.08±0.51	2.84±0.28	3.31±0.41	2.11±0.38	2.6±0.32	2.60±0.33

MH : Medtronic Hall valve, BS : Björk-Shiley valve, OC : Omnicarbon valve,
SJ : St. Jude valve, ATS : ATS valve, Sorin : Sorin valve

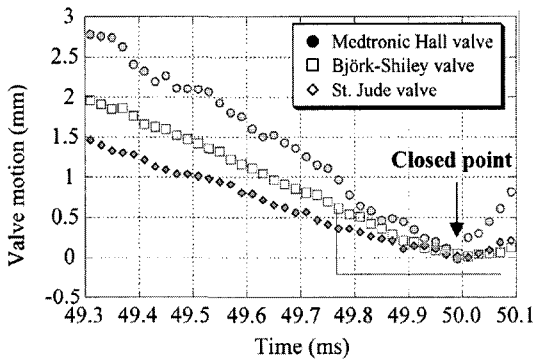

Fig. 6 Closing motion of the Medtronic Hall valve Björk-Shiley valve and St. Jude valve at heart rate of 90 beats/min

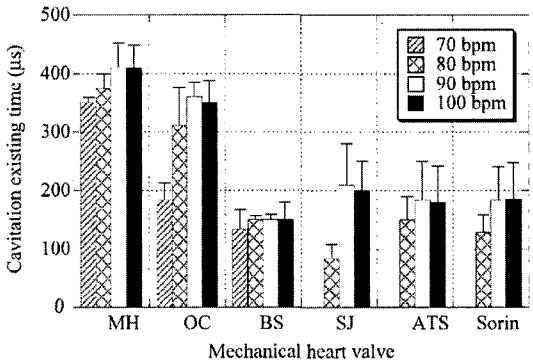

Fig. 7 Cavitation existing time of the MHV. MH : Medtronic Hall valve, BS : Björk-Shiley valve, OC : Omnicarbon valve, SJ : St. Jude valve, ATS : ATS valve, Sorin : Sorin valve

tation occurrence was alike, which were cause by squeeze flow (Fig. 5).

Figure 6 shows the valve closing motion of the monoleaflet valve (Medtronic Hall valve) and the bileaflet valve (St. Jude valve) just before closure at a heart rate of 90 beats/min. The valve closing velocity of the monoleaflet valve was faster than that of the bileaflet valve. The valve closing velocity at 0.5 ms just before closure is shown in Table 2. The valve closing velocity increased with an increase in the heart rate, with the value of the monoleaflet valves ranging from 2.0 to 4.2 m/s. Among the monoleaflet valves, the closing velocity of the Medtronic Hall valve was the fastest. The valve closing velocity of the bileaflet valves ranged from 1.5 to 2.6 m/s ; no significant difference among the bileaflet valves was observed.

Cavitation existing time of the MHV is shown in Fig. 7. At the lower heart rate of the bileaflet valve, the cavitation bubbles did not occur, and the cavitation existing time of the bileaflet valve was shorter than those of the monoleaflet valve. In particular, cavitation existing time of the Björk-Shiley valve at the higher heart rate was the shortest among the testing valves.

4. Discussion

The Björk-Shiley valve has a narrow gap between the leaflet and valve housing, as shown in Fig. 4(b), cavitation bubbles were observed at the narrow gap between the leaflet and the valve housing, which caused the venturi effect (Fig. 8 (b)). Also, in the Björk-Shiley valve, the valve stop is located on the inner side of the leaflet (Fig. 8(b)), so that the contact velocity with the valve stop was lower that the valve tip velocity. In the Björk-Shiley valve, therefore we can not ob-

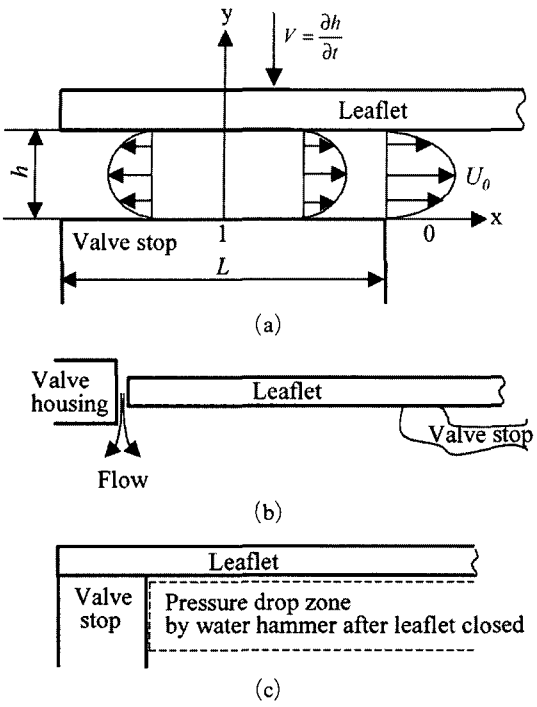

Fig. 8 Configuration of the mechanisms for cavitation in mechanical heart valve. (a) Squeeze flow, (b) Venturi effect, (c) Water hammer effect

serve the cavitation bubbles cause by squeeze flow. If cavitation was occurred by the pressure drop for water hammer (Fig. 8(c)), we might be observed cavitation bubbles on the inner side of the leaflet, however, in this study, we did not observe any cavitation bubbles on the inner side of the leaflet. Cavitation bubbles in the mono-leaflet and bileaflet valves were concentrated on the edge of the valve stop, and these were caused by squeeze flow in the narrow gap between the leaflet and the valve stop (Fig. 8(a)).

Squeeze flow is motion in the fluid volume between the contact points on the leaflet and valve stop during the final few microseconds of valve closure. The small gap in which this flow is created is referred to as the squeeze flow region. Fluid is squeezed in the outward direction away from the contact points. The valve closing velocity directly affects cavitation occurrence. We can obtain from the narrow gap between the leaflet and the valve stop the following the Reynold's equation (Schlichting, 1979),

$$\frac{\partial}{\partial x}\left(h^3\frac{\partial p}{\partial x}\right)=-12\mu\frac{\partial h}{\partial t} \tag{1}$$

From Eq. (1), we can define the following equation pressure distribution of the narrow gap between the leaflet and the valve stop center:

$$P-P_0=\frac{12\mu}{h^3}\frac{\partial h}{\partial t}\frac{1}{2}\left\{\left(\frac{L}{2}\right)^2-x^2\right\} \tag{2}$$

Applying Bernoulli's equation to points 0 and 1 of Fig. 8, we obtain P_1 of the pressure at point 1:

$$P_1=\frac{12\mu}{h^3}\frac{\partial h}{\partial t}\frac{L^2}{8} \tag{3}$$

we can obtain the squeeze flow velocity from the valve stop U_0:

$$U_0=\sqrt{\frac{3\mu}{4\rho h^3}\frac{\partial h}{\partial t}\cdot L^2} \tag{4}$$

As shown in Eq. (4), the squeeze flow velocity is proportional to the valve-closing velocity and the area of the valve stop.

Even if the closing velocity of the Bjök-Shiley valve was higher than that of the bileaflet valve, the cavitation intensity was less than that of the bileaflet valves. Assuming that the valve stop of the Bjök-Shiley valve took place in the inner side of the valve, the valve closing velocity at this point was therefore slow, and thus no cavitation bubbles were caused by squeeze flow.

Cavitation bubbles could be observed at intervals of 100-400 μs, and cavitation existing time increased with increases in the heart rate and valve closing velocity (Fig. 7). The longer interval between the existing of cavitation bubbles resulted in the growth of the cavitation bubbles and in an increase in the pressure when a bubble collapsed. It is very likely that the increasing pressure causes blood cell trauma and valve surface erosion. In this study, cavitation existing time of the Bjök-Shiley valve was the shortest. Because the valve stop of the Bjök-Shiley valve is inside the valve (Fig. 5), slow squeeze flow is generated when a valve closes. Therefore, cavitation bubbles cannot occur at the valve stop. The leaflet of the Bjök-Shiley valve was designed to have a streamlined shape. The leaflet of the Medtronic Hall

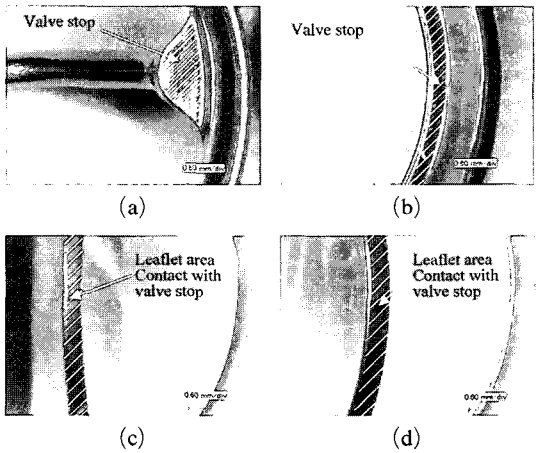

Fig. 9 Configuration of the valve stop. (a) Medtronic Hall valve, (b) Omnicarbon valve, (c) St. Jude valve, (d) Sorin valve

valve was plate-shaped, and therefore a lift force causes flutter motion of the leaflet closure. At the time of valve closure, therefore the closing velocity of the Bjök-Shiley valve has less than that of the Medtronic Hall valve (Fig. 6).

A slash mark of Fig. 9(a), (b) are show in the valve stop area, and of Fig. 9(c), (d) are shows in the leaflet area which contact with valve stop. As shown in Fig. 9, the valve stop area of the Medtronic Hall valve was greater than those of the other valves, which led to an increase in the cavitation intensity with the Medtronic Hall valve. Among the Omnicarbon valve and bileaflet valve have same level of the valve stop area (Fig. 9), however, the closing velocity of the Omnicarbon valve was more than those of the bileaflet valve, which led to an increase in the cavitation intensity with Omnicarbon valve.

6. Conclusions

Cavitation bubbles were concentrated on the valve stop and along the leaflet tip; the major cause of these cavitation bubbles was determined to be squeeze flow. From a view point of squeeze flow, the bileaflet valve with less the cavitaton intensity along the leaflet tip, assumedly preventing of blood cell damage than the monoleaflet valves. In this study provide useful information on selecting the mechanical heart valve in an electro-hydraulic total artificial heart.

References

Bluestein, D., Einav, S. and Hwang, N. H. C., 1994, "A Squeeze Flow Phenomenon at the Closing of a Bileaflet Mechanical Heart Valve Prosthesis," *J Biomech*, Vol. 27, No. 11, pp. 1369~1378.

Garrison, L. A., Lamson, T. C., Deutsch, S., Geselowitz, D. B., Gaumond, R. P. and Tarbell, J. M., 1994, "An In-vitro Investigation of Prosthetic Heart Valve Cavitation in Blood," *J Heart Valve Dis*, Vol. 3 (Suppl. I), pp. S8~S24.

Graf, T., Reul, H., Dietz, W., Wilmes, R. and Rau, G., 1992, "Cavitation at Mechanical Heart Valves Under Simulated Physiological Conditions," *J Heart Valve Dis*, Vol. 1, No. 1, pp. 131~141.

Graf, T., Reul, H., Detlefs, C., Wilmes, R. and Rau, G., 1994, "Causes and Formation of Cavitation in Mechanical Heart Valve," *J Heart Valve Dis*, Vol. 3 (Suppl. I), pp. S49~S64.

He, Z., Xi, B., Zhu, K. and Hwang, N. H. C., 2001, "Mechanisms of Mechanical Heart Valve Cavitation: Investigation Using a Tilting Disk Valve Model," *J Heart Valve Dis*, Vol. 10, pp. 666~674.

Kafesjian, R., Howanec, M., Ward, G. D., Diep, L., Wagstaff, L. S. and Rhee, R., 1994, "Cavitation Damage of Pyrolytic Carbon in Mechanical Heart Valves," *J Heart Valve Dis*, Vol. 3 (Suppl. I), pp. S2~S7.

Klepetko, W., Moritz, A., Mlczoch, J., Schurawitzki, H., Domanig, E. and Wolner, E., 1989, "Leaflet Fracture in Edward-Duromedics Bileaflet Valves," *J Thorac Cardiovasc Surg*, Vol. 97, pp. 90~94.

Knapp, R. T., Daily, J. W. and Hammitt, F. G., 1979, *Cavitation*, Iowa City: Institute of Hydraulic Research, University of Iowa.

Lee, C. S., Chandran, K. B. and Chen, L. D., 1996, "Cavitation Dynamics of Medtronic Hall Mechanical Heart Valve Prosthesis: Fluid Squeezing Effect," *J Biomech Eng*, Vol. 118, No. 1, pp. 97~105.

Makhijani, V. B., Yang, H. Q., Singhal, A. K. and Hwang, N. H. C., 1994, "An Experimental-

Computational Analysis of MHV Cavitation: Effects of Leaflet Squeezing and Rebound," *J Heart Valve Dis*, Vol. 3 (Suppl. I), pp. S35~S48.

Schlichting, H., 1979, "Boundary Layer Theory," 7th Edition. McGraw-Hill Book Co., New York.

Sneckenberger, D. S., Stinebring, D. R., Deutsch, S., Geselowitz, D. B. and Tarbell, J. M., 1996. "Mitral Heart Valve Cavitation in an Artificial Heart Environment," *J Heart Valve Dis*, Vol. 5, pp. 216~227.

Wu, Z. J., Wang, Y. and Hwang, N. H. C., 1994, "Occluder Closing Behavior: A Key Factor in Mechanical Heart Valve Aavitation," *J Heart Valve Dis*, Vol. 3 (Suppl. I), pp. S25~S34.